Batch fabrication of 50 μm thick anisotropic Nd-Fe-B micromagnets

Frederico Keller, Richard Haettel, Thibaut Devillers, Nora M. Dempsey

Batch fabrication of 50 µm thick anisotropic Nd-Fe-B micro-magnets

Frederico O. Keller, Richard Haettel, Thibaut Devillers, and Nora M. Dempsey

Univ. Grenoble Alpes, CNRS, Institut NEEL, 38000 Grenoble, France

We applied standard MEMS fabrication techniques (lithography, etching and sputtering) to the batch fabrication of out-of-plane textured 50 µm thick Nd-Fe-B micro-magnets on Si substrates of diameter 100 mm. Pre-patterning of the Si substrate serves to structure the in-plane dimensions of the micro-magnets and affords stress relief in the magnetic layer. Two protocols were applied to grow the films: a 1-step process, in which the film is directly crystallized and a 2-step process, where the film is amorphous in the as-deposited state and crystallized during a post-deposition annealing. Both processing routes result in micro-magnets with magnetic properties (texture and coercivity) comparable to sintered Nd-Fe-B bulk magnets. We report on how substrate patterning and film thickness affect the very distinctive microstructures of our films. Finally, the stray magnetic field patterns produced above these topographically patterned films was characterized by scanning Hall probe microscopy (SHPM).

I. Introduction

MICRO-Electro-Mechanical Systems (MEMS) and other micro-scale devices (µ-actuators, µ-motors, µ-generators, µ-sensors…) are applied in areas as diverse as consumer electronics, IoT networks, and biotechnology. Micro-systems that use magnetic actuation benefit greatly from down scaling [1]. To be able to produce such systems, high performance micro-magnets are needed. To date, Nd-Fe-B based sintered magnets are the most outstanding permanent magnets available [2]. However, the conventional sintering route, which results in fully dense high performance magnets, is not adapted for micro-magnet fabrication. Many fabrication methods were explored [3] and the two most promising fabrication routes to obtain integrated Nd-Fe-B micro-magnets directly on Si substrates are bonded Nd-Fe-B particles embedded in Si etched cavities [4] or sputter deposition of Nd-Fe-B films [5] combined with topographic [6] or thermomagnetic patterning [7]. The remanent magnetization of the bonded micro-magnets is limited by dilution in the binder and the isotropic character of the hard magnetic powders used. While high coercivity, highly textured thick Nd-Fe-B films were successfully deposited on metallic substrates [8], a number of groups reported a loss in both coercivity and out-of-plane c-axis texture with increasing thickness of Nd-Fe-B films deposited on metallic [9,10] and Si substrates [11]. The inclusion of spacer layers in multilayered structures ($[Nd\text{-}Fe\text{-}B/Ta]_n$, $[Nd\text{-}Fe\text{-}B/Mo]_n$, $[Nd\text{-}Fe\text{-}B/Tb]_n$,) has been shown to be effective in suppressing these losses [12-15]. However, the volume fraction of the hard magnetic phase is reduced by the introduction of the spacer layers, and processing time is increased due to the constant change of sputtering targets. Pulsed laser deposition (PLD) [16] was used to obtain very thick Nd-Fe-B films (< 160 µm) but they had low magnetization as they were isotropic, they covered only a small surface (5x5 mm^2) and they were very rough due to the presence of droplets. Here we report on the triode sputtering of 50 µm thick Nd-Fe-B micro-magnets, which maintain the excellent extrinsic properties (high remanence due to out-of-plane texture and high coercivity) reported earlier for 5 µm thick Nd-Fe-B films [5]. The batch fabrication of these thick micro-magnets on 100 mm Si substrates should facilitate their integration into MEMS.

II. Experimental details

A. Substrate patterning

Standard clean room UV-lithography was used to pattern photoresist on 100 mm (001) Si substrates. Deep Reactive Ion Etching (DRIE) was applied to anisotropically etch 55 µm deep features into the Si. Two types of patterns were etched: squares with lateral size varying from 20 to 400 µm, and 4.5 mm long stripes with width varying from 20 to 400 µm. The separation space between features is the same size as the feature, i.e., 20 µm features are 20 µm apart from each other, 30 µm features are 30 µm and so on. The etched regions will be referred as "valleys" and the non-etched regions as "hills"

B. Nd-Fe-B film deposition

High rate (15 µm/h) triode sputtering was used to deposit [Ta(0.1 µm)/Nd-Fe-B(50 µm)/Ta(0.1 µm)] trilayers onto topographically patterned Si substrates. The Nd-Fe-B layer was deposited using an alloy target of size 10 ×

10 cm^2 and composition $Nd_{16.8}Fe_{74.7}B_{8.5}$ and the substrate was rotated during deposition to favour composition and thickness homogeneity across the wafer. Two film processing routes were applied: a 1-step route in which the film was deposited at 700 °C and the $Nd_2Fe_{14}B$ phase is directly crystallized, and a 2-step route where the film is deposited at 500 °C (amorphous in the as-deposited state), requiring a post-deposition annealing to crystallize the $Nd_2Fe_{14}B$ phase. The annealing was performed on the full substrate in a Rapid Thermal Annealing (RTA) furnace, under high vacuum (10^{-6} mbar) at 600 °C, with a heating rate of 20 °C/s and a dwell time of 10 min. Hereafter, the film deposited at 700 °C will be referred as 1-step processed and the film deposited at 500 °C with subsequent annealing as 2-step processed.

C. Characterization

Microstructural characterization was carried out with a Zeiss Ultra Plus Field Emission Scanning Electron Microscope. The magnetic properties of the films were characterized using a Vibrating Sample Magnetometer (VSM), with a maximum applied field of 7.5 T. The magnetic stray field produced by the micro-magnets was characterized with an updated version of an in-house developed Scanning Hall Probe Microscope [17]. The active area of the Hall probes used here is 4×4 μm^2.

III. Results and discussion

A. Batch fabrication

We have successfully produced mechanically intact 50 µm thick Nd-Fe-B films on topographically patterned 100 mm diameter Si substrates using both the 1-step and 2-step processes. No film peel-off or substrate chipping was observed on these films. A fully processed 2-step film is shown in Figure 1.

It should be noted that if we deposit Nd-Fe-B films on non-patterned Si substrates, they peel off the substrate when the film thickness is increased beyond 10 µm. The presence of regular discontinuities and the small size of the features contribute to relieving the stress in the film, thus making it possible to grow mechanically intact Nd-Fe-B films up to 50 µm in thickness.

B. Microstructural characterization

Figure 2 shows cross-section SEM images of Nd-Fe-B deposited on regions with different dimensions of etched features. Note that in the first two rows, the scalebar is 50 µm, and for the subsequent rows it is 20 µm. The images were made on fractured cross sections of areas containing stripes. It can be seen that deposit on the hills have the expected thickness of 50 µm, while for deposit in the valleys the film thickness and its shape depend on the distance between adjoining hills. This variable filling of the valleys is caused by shadowing of particle flux and will depend on the Si step size (depth etched into the substrate), film thickness and angular distribution of sputtered species. The shadowing effect is more pronounced when the valley width is small compared to the step size and film thickness. We can also see in the same figure that deposition on the sidewalls results in the width of the deposit on the "hills" being wider than the underlying Si pillars. For a 50 µm thick deposit, a sidewall lateral growth of about 10 µm is found for all "valley" widths.

Figure 3 shows the microstructure of relatively wide features (400, 200 and 100~µm width). A homogeneous grain structure is observed through the film thickness, and represents most of the film for these features. In the 1-step film, out-of-plane elongated coarse grains are observed. However, it is difficult to precisely determine the grain size and shape due to the mixture of transgranular and intergranular fracture. A fine-grained microstructure was found in the 2-step film, with quasi-equiaxed grains measuring between 200-500 nm. The difference in the microstructure of the two film types studied here is consistent with what we reported for 5 µm thick films, where we showed that films deposited in the crystallized state have out-of-plane oriented long columnar grains while films crystallized during a post-deposition anneal have much finer quasi-equiaxed grains [5].

A particular microstructure develops in the vicinity of the silicon steps (Figure 4). In the 1-step film, grains growing on the sidewall have an oblique angle with respect to the substrate plane. For the 2-step film, the orientation of the grains crystallized in the sidewalls is not evident, as they are almost equiaxed. Nevertheless, we see columnar grains oriented with their long axis close to the in-plane direction in the boundary region between the sidewall and "hill/valley" deposit.

C. Magnetic properties

In-plane (ip) and out-of-plane (oop) *M(H)* curves of 1-step and 2-step films are shown in Figure 5. In both films, a significant difference in magnetization values of ip and oop curves is observed. From the oop *M(H)* curve, $M_{0T}/M_{7.5T}$ values of 0.79 for 1-step and 0.85 for 2-step films were obtained. Given the complexity of shapes seen in Figure 2, it was not possible to precisely calculate the film volume to obtain an estimative of absolute

magnetization (in Tesla). Nevertheless, the difference seen in ip and oop *M(H)* curves proves the strong out-of-plane c-axis texture obtained in these films.

The out-of-plane coercivity of the 1-step film is 1.2 T, while the 2-step film reaches 2.2 T. The relatively high values of coercivity achieved for both film types is attributed to the formation of a Nd-rich grain boundary phase identified by Transmission Electron Microscopy imaging and atom probe analysis of such films [18]. The Nd-rich phase forms thanks to the use of a target which is relatively rich in Nd, and it serves to partially decouple neighboring grains. The higher value of coercivity in the 2-step processed film is attributed to its finer grain size, which favors higher coercivity. Indeed, the value of coercivity exceeds that reported for bulk sintered magnets, for which the lower limit of grain size reported is 1 µm [19]. The above described difference in microstructure of the two films is reflected in the initial magnetization curves of the samples in the virgin state. The coarse grained film (1-step) shows high initial magnetic susceptibility, whereas a clear two-stage magnetization is observed in the fine-grained film (2-step). The two-stage behaviour of the initial magnetization is attributed to the presence of multi-domain (high susceptibility) and single domain (low susceptibility) $Nd_2Fe_{14}B$ grains [5].

D. Stray field measurements

Stray field measurements were performed using the Scanning Hall Probe Microscope (SHPM) on topographically patterned 50 µm thick Nd-Fe-B stripe arrays obtained from 1-step and 2-step processed films. The stripes have a constant length of 4.5 mm and variable widths in the range of 20-400 µm. The SHPM scans were performed in the central region of the stripes over an area of 1×5 mm^2, and at 30 and 50 µm from the top surface of the micro-magnets.

Figure 5 shows 2D maps and 1D profiles of the out-of-plane component of stray field (B_z) for 1-step and 2-step films. When analyzing the 2D maps, we can see a difference in colour contrast between 1-step and 2-step processed films. This difference in field intensity is even clearer when we analyze the 1D profiles extracted from the 2D measurements. The 1D profile reveals that the maximum B_z generated by the 1-step film at 30 µm is 85 mT, while for the 2-step it reaches 108 mT. In both cases, the maximum B_z is observed over the 200 µm wide stripes.

Depending on the targeted application, the lateral size and thickness of the magnets would need to be tuned to optimize the magnetic stray field at the operating distance. An alternative to the presented approach is to remove the magnets on top of the hills by a chemical mechanical polishing step in order to only use the magnets buried in the valleys. This approach is currently being developed.

IV. Conclusion

We have shown that it is possible to maintain excellent extrinsic magnetic properties (high remanence due to out-of-plane texture and high coercivity) in triode sputtered Nd-Fe-B films of thickness up to 50 µm. Topographic patterning of the silicon substrate prior to film deposition induces the emergence of a magnetic stray field and very importantly it promotes stress relief, which allows the growth of thick (>10 µm) Nd-Fe-B films without peel off. Two protocols were applied to grow the 50 µm thick films: a 1-step process, in which the film is directly crystallized and a 2-step process, where the film is amorphous in the as-deposited state and crystallized during a post-deposition anneal. The finer grain size of the 2-step processed film results in a high value of coercivity. The successful batch fabrication of mechanically intact 50 µm thick Nd-Fe-B micro-magnets on 100 mm diameter Si substrates represents a milestone on the route to their future integration into magnetic micro-systems. To probe the impact of the use of pre-patterned substrates on local variations in texture, we will now carry out quantitative texture analysis using Electron BackScatter Diffraction (EBSD). We will also compare stray field measurements made using SHPM with field profiles predicted by modelling. Finally, we will prepare new test structures in which the feature size is fixed at a given value in a given die, to allow assessing the impact of feature size on texture and eventually coercivity, as measured by VSM-SQUID.

Acknowledgment

The authors would like to thank Simon le Denmat, Roman Kramer and Klaus Hasselbach (Institut Néel) for their development of the Scanning Hall Probe Microscope used in this study and their assistance with its use. This work was supported in part by the French National Research Agency (ANR) through the ANR-POMADE (16-CE09-0019) project.

REFERENCES

[1] O. Cugat, J. Delamare, and G. Reyne, "Magnetic micro-actuators and systems (MAGMAS)," *IEEE Trans. Magn.*, vol. 39, no. 6, pp. 3607–3612, Nov. 2003.

[2] O. Gutfleisch, M. A. Willard, E. Brück, C. H. Chen, S. G. Sankar, and J. P. Liu, "Magnetic Materials and Devices for the 21st Century: Stronger, Lighter, and More Energy Efficient," *Adv. Mater.*, vol. 23, no. 7, pp. 821–842, Feb. 2011.

[3] D. P. Arnold and Naigang Wang, "Permanent Magnets for MEMS," *J. Microelectromechanical Syst.*, vol. 18, no. 6, pp. 1255–1266, Dec. 2009.

[4] T. Lisec *et al.*, "Integrated High Power Micro Magnets for MEMS Sensors and Actuators," in *2019 20th International Conference on Solid-State Sensors, Actuators and Microsystems & Eurosensors XXXIII (TRANSDUCERS & EUROSENSORS XXXIII)*, 2019, vol. 5, no. June, pp. 1768–1771.

[5] N. M. Dempsey, A. Walther, F. May, D. Givord, K. Khlopkov, and O. Gutfleisch, "High performance hard magnetic NdFeB thick films for integration into micro-electro-mechanical systems," *Appl. Phys. Lett.*, vol. 90, no. 9, 2007.

[6] A. Walther, D. Givord, N. M. Dempsey, K. Khlopkov, and O. Gutfleisch, "Structural, magnetic, and mechanical properties of 5 μm thick SmCo films suitable for use in microelectromechanical systems," *J. Appl. Phys.*, vol. 103, no. 4, 2008.

[7] F. Dumas-Bouchiat *et al.*, "Thermomagnetically patterned micromagnets," *Appl. Phys. Lett.*, vol. 96, no. 10, pp. 1–4, 2010.

[8] B. A. Kapitanov, N. V. Kornilov, Y. L. Linetsky, and V. Y. Tsvetkov, "Sputtered permanent Nd-Fe-B magnets," *J. Magn. Magn. Mater.*, vol. 127, no. 3, pp. 289–297, Oct. 1993.

[9] S. Yamashita, J. Yamasaki, M. Ikeda, and N. Iwabuchi, "Anisotropic Nd-Fe-B Sputtered Thin Film Magnets," *IEEE Transl. J. Magn. Japan*, vol. 7, no. 1, pp. 45–50, Jan. 1992.

[10] S. . Piramanayagam, M. Matsumoto, and A. Morisako, "Thickness dependence of magnetic properties of NdFeB thin films with perpendicular magnetic anisotropy," *J. Magn. Magn. Mater.*, vol. 212, no. 1–2, pp. 12–16, Mar. 2000.

[11] Q. Yao, W. Liu, W. B. Cui, F. Yang, X. G. Zhao, and Z. D. Zhang, "Growth mechanism and magnetic properties for the out-of-plane–oriented Nd–Fe–B films," *J. Mater. Res.*, vol. 24, no. 09, pp. 2802–2812, Sep. 2009.

[12] N. Gennai, M. Uehara, M. Fujiwara, and T. Tanaka, "Investigation of microstructure of Nd-Fe-B/Ta multilayered films by scanning transmission electron microscopy," *Thin Solid Films*, vol. 509, no. 1–2, pp. 102–106, 2006.

[13] W. Liu, S. Suzuki, and K. Machida, "Orientation and Magnetic Properties of the Thick Multilayered [NdFeB x /Tb y] n Films," *Jpn. J. Appl. Phys.*, vol. 46, no. 7A, pp. 4113–4116, Jul. 2007.

[14] Y. Jiang *et al.*, "Fabrication of a vibration-driven electromagnetic energy harvester with integrated NdFeB/Ta multilayered micro-magnets," *J. Micromechanics Microengineering*, vol. 21, no. 9, 2011.

[15] M. Grigoras *et al.*, "Layering influence on Nd agglomeration and hard magnetic properties of Mo/NdFeB/Mo thick films," *Thin Solid Films*, vol. 665, no. September, pp. 68–74, Nov. 2018.

[16] M. Nakano *et al.*, "Nd–Fe–B Film Magnets With Thickness Above 100 μm Deposited on Si Substrates," *IEEE Trans. Magn.*, vol. 51, no. 11, pp. 1–4, Nov. 2015.

[17] G. Shaw, R. B. G. Kramer, N. M. Dempsey, and K. Hasselbach, "A scanning Hall probe microscope for high resolution, large area, variable height magnetic field imaging," *Rev. Sci. Instrum.*, vol. 87, no. 11, pp. 1–24, 2016.

[18] N. M. Dempsey *et al.*, "High-coercivity Nd-Fe-B thick films without heavy rare earth additions," *Acta Mater.*, vol. 61, no. 13, pp. 4920–4927, 2013.

[19] J. Li, H. Sepehri-Amin, T. Sasaki, T. Ohkubo, and K. Hono, "Most frequently asked questions about the coercivity of Nd-Fe-B permanent magnets," *Sci. Technol. Adv. Mater.*, vol. 22, no. 1, pp. 386–403, 2021.

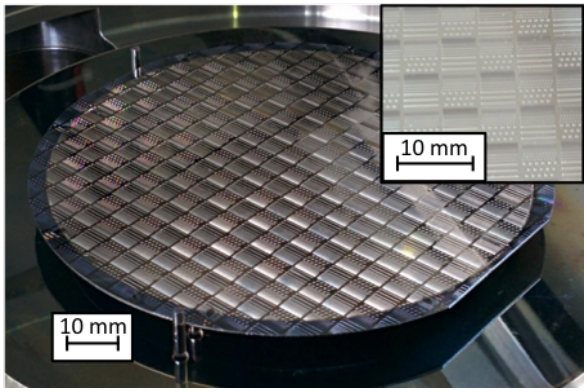

Fig. 1. Optical image of a 2-step processed 50 µm thick Nd-Fe-B film deposited onto a topographically patterned 100 mm diameter Si substrate. Inset: optical image showing the features.

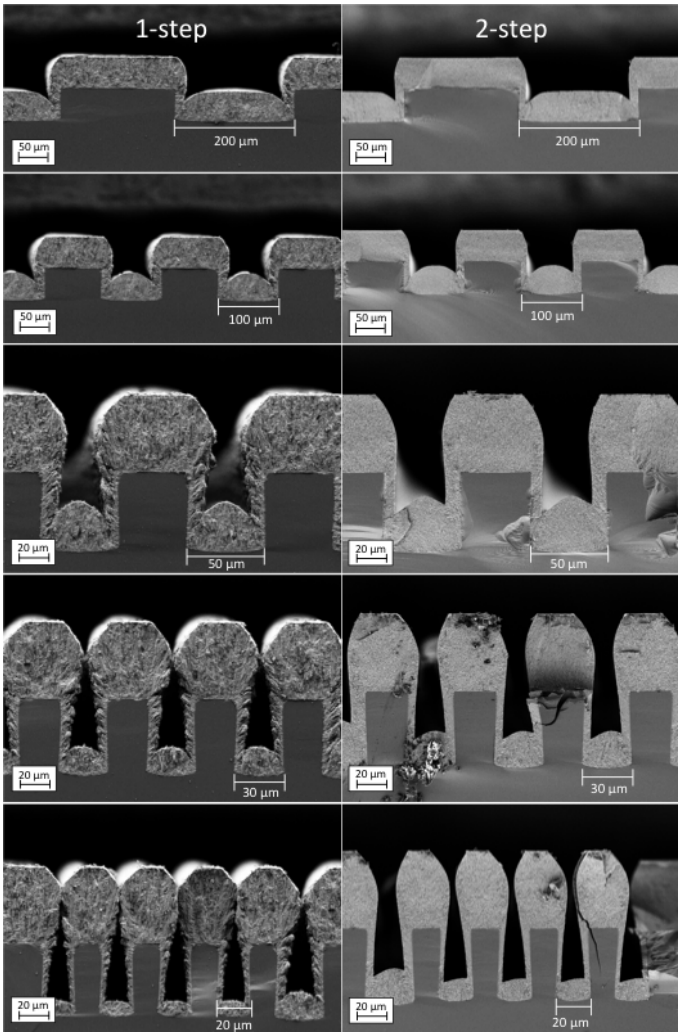

Fig. 2. SEM cross-section images of 50 µm thick Nd-Fe-B film deposited onto patterned Si substrates. Left column: 1-step processed, right column: 2-step processed. Hills and valleys have the same width (from top to bottom: 200, 100, 50, 30, 20 µm)

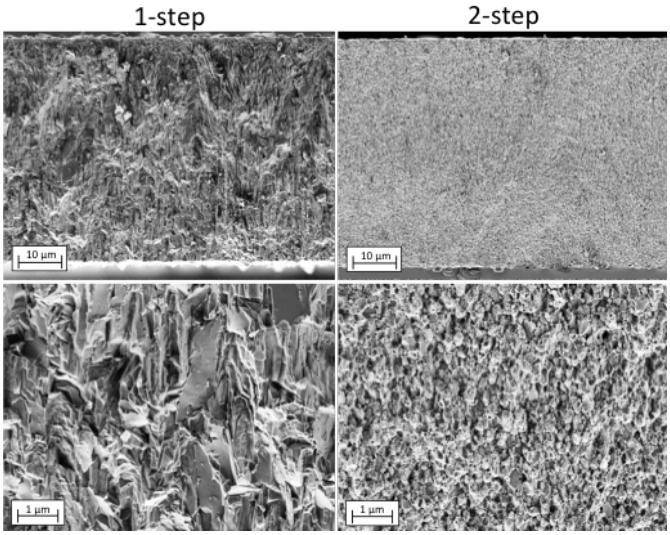

Fig. 3. SEM cross-section images showing the microstructure of 1-step (left) and 2-step (right) processed films at low (top) and high (bottom) magnification.

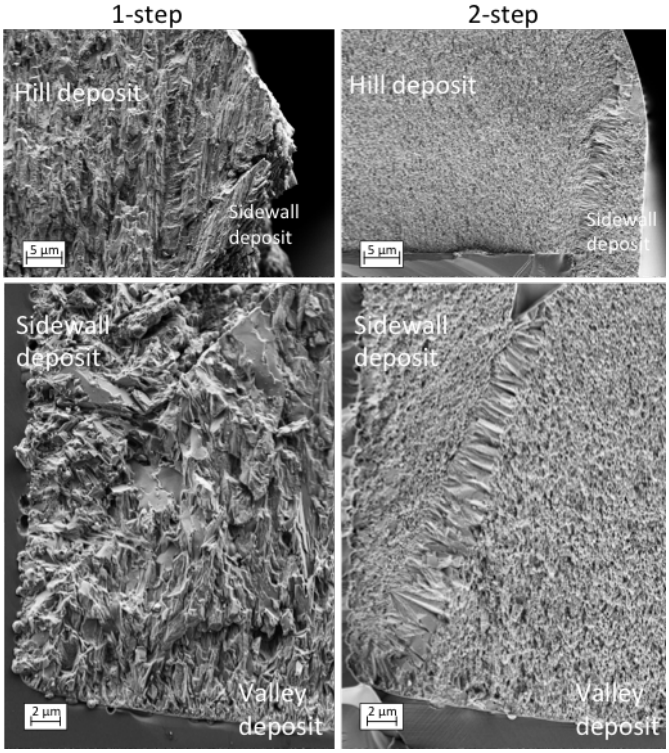

Fig. 4. SEM cross-section images showing the microstructure developed on the regions in the vicinity of the Si step.

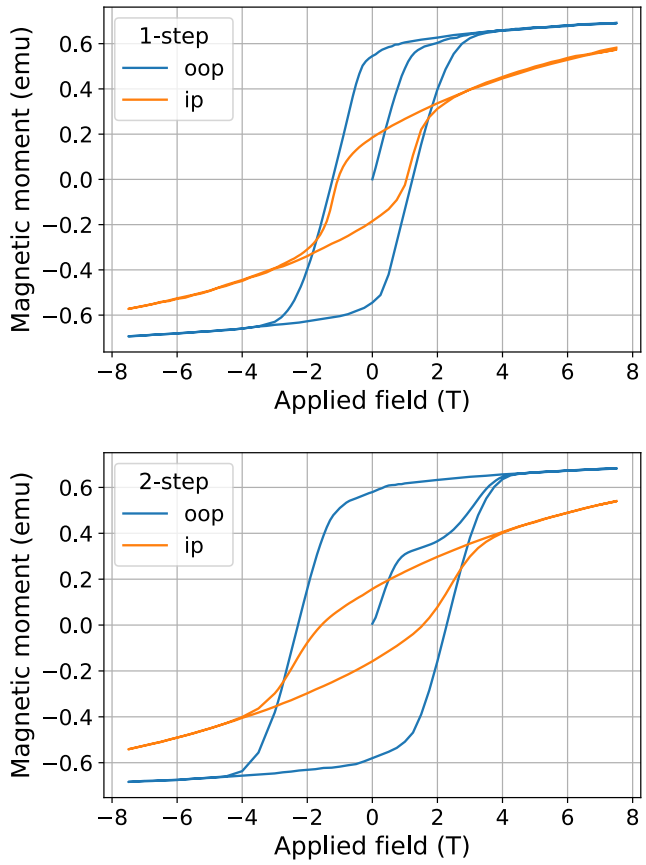

Fig. 5. In plane (ip) and out-of-plane (oop) measurement of magnetic moment as a function of applied field for 1-step (top) and 2-step (bottom) processed films.

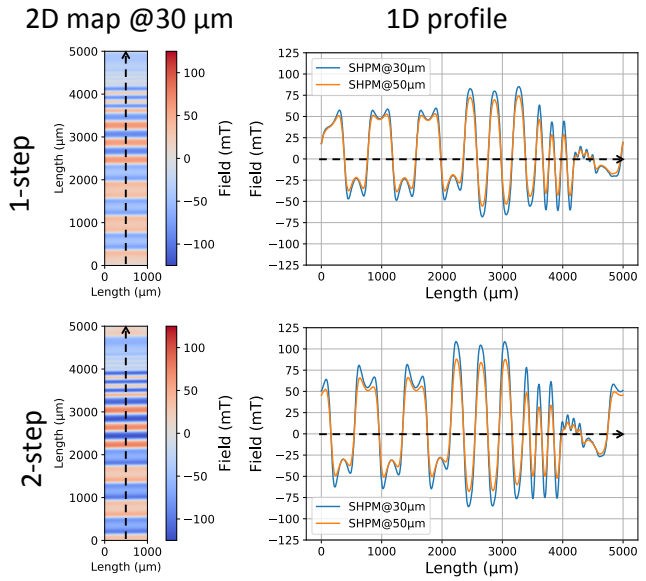

Fig. 6. 2D Maps and 1D profiles of the out-of-plane component of the magnetic stray field (B_z) for 1-step (top) and 2-step (bottom) processed samples. The dashed arrows indicate the scan direction.